Chemical Engineering Journal 525 (2025) 170385

Contents lists available at ScienceDirect

Chemical Engineering Journal

journal homepage: www.elsevier.com/locate/cej

Integrating optimal design of experiments and superstructure optimization under uncertainties for the design of membrane processes

Stefanie Kaiser [a,*], Stefan Schlüter [b], Mirko Skiborowski [c], Sebastian Engell [a]

[a] Department of Biochemical and Chemical Engineering, TU Dortmund University, Emil-Figge-Straße 70, 44227, Dortmund, Germany
[b] Laboratory of Fluid Separations, Department of Biochemical and Chemical Engineering, TU Dortmund University, Emil-Figge-Straße 70, 44227, Dortmund, Germany
[c] Institute of Process Systems Engineering, Hamburg University of Technology, Am Schwarzenberg-Campus 4, 21073, Hamburg, Germany

ARTICLE INFO

Keywords:
Membrane Processes
Process Synthesis
Uncertainty
Design of Experiments
Superstructure Optimization

ABSTRACT

Membrane processes are attractive options for fluid separations as they enable highly selective separations under mild process conditions. The design and evaluation of membrane processes is however a complex task, due to the large variety of different separation principles and corresponding types of membrane processes, a variety of different membrane materials, and alternative process structures, as well as the limited availability of data and models that is especially a hurdle in the early-stage design of chemical processes. A model- and optimization-based approach can help to design membrane separation processes systematically but requires the determination of a sufficiently accurate process model that usually requires time-consuming experimental work. In the early stage of process design, there are still many options regarding the process structure and operating parameters, and it is desirable to focus the experimental and modelling efforts only on promising process variants and operating conditions. For this purpose, the current work presents an integrated methodology that enables the application of optimization-based methods in early phase process design applied to a reaction-separation process. The application focusses on the selection and design of the membrane separation as an important aspect of the overall flowsheet. By performing a superstructure optimization in which uncertainties are explicitly considered, a set of promising flowsheet variants can be selected. Instead of a separated design of experiments for the model identification, an integral approach is pursued by selecting the most informative experiments on the basis of the impact of the model uncertainties on the design decisions, in order to quickly determine the most relevant parameters. In the specific case study, the methodology is used for the conceptual design of a membrane process where the membrane is used to separate a co-product from a complex reaction mixture while retaining the expensive homogeneous catalyst. Using the integrated approach only one set of experiments in addition to the initial screening experiments is necessary to identify the optimal flowsheet for the case study.

1. Introduction

During the early-stage process design of chemical processes, decisions on the reaction pathways, catalysts, solvents and on the process units and their mode of operation, e.g. stirred tank reactors operated continuously or in batch mode or tubular reactors, and on the choice of separation units as well as their interconnections (linear structures, recycle streams, withdrawal of side streams) have to be made. The decisions that are fixed in this stage do not only provide the scope for the subsequent detailed design of the process and its operation, but also have a major influence on the final production cost, as they may account for 80 % of the entire process costs [1]. The uncertainties about the production cost are usually larger than 10 %.

Early-stage design approaches can generally be divided into heuristic and optimization-based methods. Heuristic methods are based on expert knowledge, and are either condensed into simple rules of thumb [2] or implemented in dedicated expert systems [3]. The overall process design problem is usually decomposed into a sequence of smaller sub-problems following the hierarchical approach proposed by Douglas [4]. This approach has the disadvantage that synergies between the different process sections are difficult to exploit as each unit is designed individually instead of considering the complete process. In industrial practice, heuristic methods based on expert knowledge are used in a combination with flowsheet simulation by which the designer explores

* Corresponding author.
E-mail address: stefanie2.kaiser@tu-dortmund.de (S. Kaiser).

https://doi.org/10.1016/j.cej.2025.170385
Received 4 May 2025; Received in revised form 1 October 2025; Accepted 31 October 2025
Available online 5 November 2025

the part of the design space that he/she considers to be the most promising.

1.1. Superstructure optimization

Optimization-based methods can either be used to optimize the parameters of heuristically chosen configurations or include the choice of the process units and their interconnections by means of superstructure optimization. These methods are based on models of the chemical and physical phenomena of relevance that occur within the process units. Even for a fixed process structure, these problems are usually strongly nonlinear and, depending on the objective function which is optimized, may be multi-modal, requiring exact or meta-heuristic global optimization methods and a significant computational effort [5,6].

When the structure and the parameters of the process are optimized simultaneously, first a superstructure of the possible unit operations or pieces of equipment is set up, and among the possible combinations, the best process is selected by optimizing the structural, sizing and operational parameters. Generating the superstructure requires careful preselection of unit operations or pieces of equipment, but also approaches to represent more flexible structures exist [7]. Due to the discrete decisions on certain unit operations the resulting problems are usually formulated as mixed-integer nonlinear programming (MINLP) problems, or less frequently as generalized disjunctive programming (GDP) problems.

The inherent non-convexities in these problems present considerable solution challenges. While rigorous process models and deterministic gradient-based optimization methods have been applied for specific problems, such as the synthesis and design of simple and intensified distillation processes [8], they remain difficult to apply for general process synthesis problems. Therefore, stochastic or hybrid methods are frequently employed. For the optimization of reactive distillation processes, Urselmann et al. [5] developed a memetic algorithm that integrates a mathematic programming solver with an evolutionary algorithm to handle the discrete decisions. Skiborowski et al. [9] used a hybrid algorithm for the optimization of the separation process of ethanol and water, which was more recently compared with a global deterministic optimization for a simple column by Kruber et al. [10], who furthermore extended the application to intensified extractive distillation processes.

The models of the different process units that are involved in a flowsheet can usually be taken from the literature and available databases on physical properties for standard operations and frequently occurring mixtures, as embedded in commercial process simulators such as Aspen Plus. However, these model libraries still lack certain models for more innovative processes, such as e.g., membrane separations, which have to be developed during the process design stage. Usually, for such processes established model structures are employed in user-defined models for which the model parameters are initially fitted to data from laboratory experiments [11]. These experiments require a significant effort which should be limited to the necessary extend in order to save resources and speed up the development process. Therefore, instead of broad experimental studies, dedicated to the development of very accurate models of process units and materials, such as membrane materials, the experimental investigations should focus on the process units and operating conditions that are relevant for the best flowsheet. As these are not known in the initial phase, an integrated approach of model development and process optimization can be applied, in which the selection of the most promising flowsheet is based on relatively coarse models which are only refined up to the point where a choice can be made, after which more accurate models are determined for the remaining relevant process units under the operating conditions which result from the first optimizations.

Model parameter uncertainties influence the optimal design decision and should be taken into account in the superstructure optimization. Grossmann and Sargent [12] first considered a scenario representation of the uncertain model parameters and applied optimization under uncertainty to superstructure optimization, separating design and operational degrees of freedom. Paules and Floudas [13] extended the optimization under uncertainties to integer variables. Superstructure optimization is mostly pursued via the formulation and solution of MINLP problems and especially if the optimization is performed under uncertainties it leads to large optimization problems. Pintaric and Kravanja [14] presented an algorithm to solve large MINLP problems stochastically under uncertainty. Steimel and Engell [15] separated design and operational degrees of freedom where the design degrees of freedom have to be decided on under uncertainty whereas the operational parameters can be adapted to the realization of the uncertainties during operation and are optimized individually for each scenario of the uncertain parameters, leading to a two-stage pseudo-stochastic optimization problem. The first stage of the optimization problem was solved using an evolutionary algorithm and the scenario dependent second stage variable were optimized using an NLP solver.

1.2. Optimization-based design of membrane networks

The design of membrane networks via superstructure optimization has been tackled by several researchers. Skiborowski et al. [16] provide an overview on superstructure optimization for the design of membrane assisted distillation processes and apply a rigorous optimization approach to several case studies, using a polylithic solution strategy, in which the overall problem is first decomposed into smaller subproblems that are solved individually for the initialization of the full MINLP problem, which is subsequently solved simultaneously as a series of successively relaxed NLP problems. Scharzec et al. [17] extended this work to intensified pervaporation-distillation processes, promoting an initial screening under the assumption of a perfect membrane separation, in order to evaluate the maximum potential of a membrane-assisted process and narrow down the operating conditions for a subsequent experimental screening. The most recent work by Chia et al. [18] applies a hybrid solution strategy for multi-objective optimization combining a superstructure model in gPROMS and the stochastic NSGA-II solver.

Scharzec et al. [19] designed a membrane configuration with three stages for the removal of a by-product of a homogeneously catalyzed reductive amination process. The embedding of data-driven surrogate models in the optimization of membrane networks has gained attention in the past years. Rall et al. [20] used surrogate models that are based on ion transport models that are valid on a nano-scale for the superstructure optimization of membrane processes and applied these models for a simultaneous rational design of ion separation membranes and processes, which also takes into account the synthesis of a suitable membrane. Di Martino et al. [21] designed a membrane network for the desalination of water using superstructure optimization. They modeled the membranes using artificial neural networks (ANNs) that were trained based on industrial scale plant data. However, none of these works considered the simultaneous design of the membrane network and of the other process units that can exploit synergistic effects.

The modelling of membrane processes is difficult, because due to the large variety of membrane materials and types there is no standard modelling approach. Reliable predictions typically require to parameterize the models based on experimental data at relevant operating conditions for several candidate membranes, leading to a significant experimental effort. This is especially true for applications of organic solvent nanofiltration, where the space of solvents, solutes and membranes is very large, with strong interactions between the membrane types, solvents and solutes, especially for polymeric membranes [22]. Despite advances in the availability of data [23,24], and the development of data-driven models for the prediction of the flux and the rejection of specific membranes [25–28] experiments are still essential, especially for complex mixtures. Therefore, it is proposed here to follow a sequential approach where first a superstructure optimization is performed using coarse models which leads to significant uncertainties in

the prediction of the performance, and then the models are step-wise refined for those configurations which have not been excluded because even in the best case they perform worse than others in the worst case.

Such a methodology for fast, model-based process design was recently proposed by Kaiser and Engell [29]. It integrates superstructure optimization under uncertainty with optimal design of experiments. Those parameters that influence the optimal design decision most are identified and their estimation is improved using optimally designed experiments. In [29] an in-silico study of a complex multi-phase reaction system was reported, in which the methodology was used to plan experiments for refining the parameters of the kinetic models. It was shown that the experimental effort can be reduced significantly, and the process design can be accelerated. The aim of this contribution is to extend the proposed methodology to the design of a multiphase reaction system that includes a membrane separation unit for which the membrane material and the connection structure of several possible stages must be selected. Here we include the design and execution of laboratory experiments which are used to improve the estimation of the parameters of the membrane models. This not only shows the transferability of the methodology to more complex flowsheets but also demonstrates the applicability to the design of real experiments. As the application, the homogenously catalyzed hydroaminomethylation of 1-decene in a thermomorphic multiphase system is considered where a membrane unit is used to separate the by-product water from the stream that leaves the reactor to avoid its accumulation via the recycle stream. Phase separation induced by a temperature shift is used to minimize the loss of the expensive homogeneous catalyst. The goal is an economically optimal process that achieves high reaction yields and a small loss of catalyst at the same time. The quality of the models that are used for the process design is improved step-wise to the extent necessary to take a decision about the process structure, avoiding unnecessary experimental work.

In Section 2, the methodology for integrated process design is presented with focus on the superstructure optimization, the identification of parameters influencing the optimal design decision and the optimal experimental design. In Section 3, the process model of the process under consideration is described. An overview about the laboratory experiments is given in Section 4 and the superstructure optimization combined with optimal experimental design is presented in Section 5. The results are presented in Section 6, which also contains the main conclusions of the paper and directions for future research.

2. Integrated design approach

The methodology proposed in [29] is depicted in Fig. 1. From first screening experiments, the model parameters of the unit models of a predefined superstructure are estimated, if the models are not available. Based upon these models for the different process units with the estimated parameters and their uncertainties, superstructure optimization under uncertainties is performed for a number of discrete scenarios of the uncertain model parameters within their confidence intervals. The optimization is performed for the complete flowsheet to consider synergies between the different unit operations. A specific feature of our approach is that two-stage optimization is employed where the operational degrees of freedom are recourse variables that can be adapted to the realization of the uncertainties (the values of the model parameters) but the structural parameters, e.g. the choice of a membrane material, are fixed for all scenarios.

The goal of the integrated design is to determine the structural parameters. If the objective values of the superstructure optimization under uncertainties overlap for different design alternatives, the models are refined for all those structures that cannot be excluded as inferior for all parameter values from the optimization, based on additional experiments. As not all model parameters usually are equally relevant for the decision on the optimal design, the most influencing parameters are identified by performing a discrimination analysis with subsequent computation of the partial dependences. Model-based optimal design of experiments is then used to plan experiments that provide the most information about the relevant parameters. After executing the planned experiments, the measurements are used to either validate or adapt the chosen model structures and to update their parameters and the ranges of their uncertainties. This iterative procedure is repeated until one structural process alternative can be identified as optimal for all realizations of the discrete scenarios. This configuration will then be tested in larger set-ups, e.g. in mini plants or at pilot plant scale which provides information that can be used to further adapt or extend the models to obtain a more reliable design and estimation of the expected performance of the process. The estimation of the performance can also be done using iterative online optimization with or without model adaptation [30–32].

In the following sections, the main elements of the methodology are

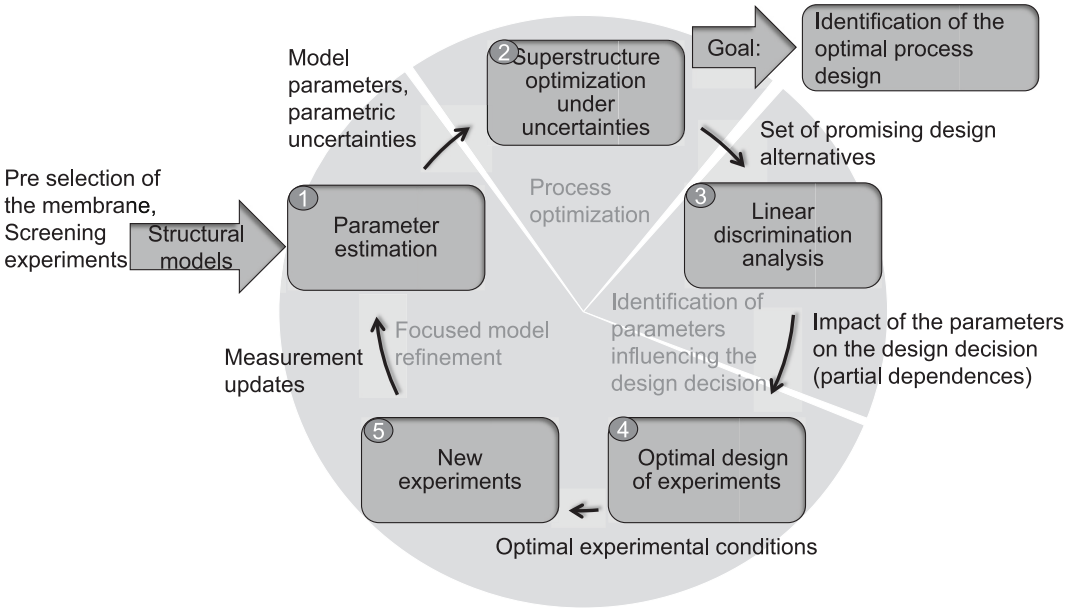

Fig. 1. Integrated methodology for optimization-based process design adapted from [29].

presented, including the superstructure optimization under uncertainties, the identification of parameters influencing the design decision and the optimal design of experiments.

2.1. Superstructure optimization under uncertainties

Superstructure optimization under uncertainties is implemented as a two-stage pseudo-stochastic programming problem. The underlying assumption is that some design variables cannot be changed after the process has been built. These design decisions may be of discrete or continuous nature (number of trays of a column, number of stages of a membrane separation, sizes of the membranes etc.). Other variables, which are further referred to as operational parameters, can be adjusted during the operation of the process by either the operator or a control and optimization system. These variables are the recourse variables in the two-stage optimization and typically are temperature set-points, pressures and flow rates. Under the assumption that the uncertainties can be represented by a finite set of discrete scenarios with different probabilities, the process synthesis problem can be formulated as the following two-stage optimization problem [15]:

$$\begin{aligned} \min_{y_d, y_c, x_\omega} \; & G(y_d, y_c) + \sum_{\omega=1}^{\Omega} \pi_\omega F_\omega(y_d, y_c, x_\omega, z_\omega) \\ \text{s.t.} \quad & g(y_d, y_c, x_\omega, z_\omega) \le 0 \\ & f(y_d, y_c, x_\omega, z_\omega) = 0 \\ & y_{d,L} \le y_d \le y_{d,U} \\ & y_{c,L} \le y_c \le y_{c,U} \\ & x_{\omega,L} \le x_\omega \le x_{\omega,U} \\ & z_{\omega,L} \le z_\omega \le z_{\omega,U} \\ & y_d \in \mathbb{Z}^{n_d}, y_c \in \mathbb{R}^{n_c}, x_\omega \in \mathbb{R}^{n_x}, z_\omega \in \mathbb{R}^{n_z} \end{aligned} \tag{1}$$

The objective function (1) consists of two terms. The first term accounts for the cost for fixing the discrete (y_d) and continuous (y_c) first stage decisions, i.e. the CAPEX related cost. The second term accounts for the operational cost (energy, materials) taking the second stage decision into account, formulated as a weighted summation over the Ω discrete scenarios using the weighting factors π_ω. A symmetric distribution of the uncertain parameters within the 95 % confidence interval of the parameters is assumed. The optimization problem is solved subject to inequality constraints, which specify feasible ranges of equipment sizes, operational limits, and product specifications. The model equations are formulated as equality constraints. Physical limitations or validity constraints of the model equations lead to lower and upper bounds for the continuous and discrete design decisions (y_d and y_c), the recourse variables (x_ω) and the implicit variables (z_ω).

The optimization problem is a large MINLP due to the presence of the different scenarios and is solved using the superstructure optimization framework (FSOpt) that was developed by Steimel and Engell [15,33]. In this framework, the first stage variables are optimized using a hybrid evolutionary algorithm and the scenario dependent operational variables are optimized for fixed first stage variables using the rigorous nonlinear programming solver (IPOPT) [34].

2.2. Optimal design of experiments

Model-based optimal design of experiments (mb-ODoE) is based on the idea to maximize the information content of experiments to optimize the resulting accuracy of estimated model parameters and/or to determine which model structure represents a given system best [35]. This leads to computationally very demanding problems especially for dynamic systems [36] and efficient numerical techniques are still under development (see e.g. [37]).

In mb-ODoE, the available knowledge at a certain stage of the model development process is used by predicting the gain of information of a potentially performed experiment using the model equations. The information content can be approximated based on the linearization of the propagation of the uncertainty of the measurements to the parameter estimates according to eq. (2). The covariance matrix of the parameters $\boldsymbol{V}$ results from the sensitivity matrix $\boldsymbol{Q}$ that depends on the estimated model parameters $\widehat{\boldsymbol{\Theta}}$ and the experimental design $\boldsymbol{u}$ and the covariance matrix of the measurements $\boldsymbol{\Psi}$ [35]:.

$$\boldsymbol{V}(\widehat{\boldsymbol{\Theta}}, \boldsymbol{u}) = \left(\boldsymbol{Q}^T \boldsymbol{\Psi}^{-1} \boldsymbol{Q}\right)^{-1}. \tag{2}$$

The sensitivity matrix $\boldsymbol{Q}$ contains the sensitivity coefficients of the predictions of the measurements by the model $\hat{y}$ with respect to the model parameters:

$$\boldsymbol{Q} = \left(\nabla_\Theta \hat{\boldsymbol{y}}^T\right)^T = \begin{bmatrix} \frac{\partial \hat{y}_1}{\partial \Theta_1} & \cdots & \frac{\partial \hat{y}_1}{\partial \Theta_p} \\ \vdots & \ddots & \vdots \\ \frac{\partial \hat{y}_{n_y}}{\partial \Theta_1} & \cdots & \frac{\partial \hat{y}_{n_y}}{\partial \Theta_p} \end{bmatrix}. \tag{3}$$

It is assumed that the measurements are unbiased and that the parameters are independent of each other [35].

The maximization of the gain of information is equivalent to the minimization of the confidence intervals of the parameters which can be expressed as the minimization of a suitable scalar measure of the size of the covariance matrix $\boldsymbol{V}$. Commonly used measures are the determinant (D-criterion), the smallest eigenvalue (*E*-criterion) or the trace (A-criterion) of $\boldsymbol{V}$ [35]. In this work, the A-optimal design of experiments is used because it enables to include a weighting of the parameters according to their impact on the process design.

As the uncertain parameters usually have a different impact on the selection of the optimal process configuration, the experiments should be planned such that they are focused on the determination of the most relevant parameters. Optimal experimental design that focuses on obtaining reliable simulation results has been investigated in previous research. Recker et al. [38] used a weighting of the parameters in an A-optimal design, where the weights are computed in a previous step as the sensitivities of a scalar quality parameter of the process simulation. Fleitmann et al. [39] introduced a new criterion for ODoE (C-criterion), where the first order sensitivity of a scalar indicator of the result of the process simulation is incorporated in the objective function to account for the importance of the model parameters. These methods all consider the impact of the uncertain model parameters on a measure of the accuracy of the output of simulation or optimization but are not necessarily suitable for the determination of the parameters that influence the discrete design decisions most. Some parameters may have a strong influence on the process performance, e.g. the product yield, but not on the decision on which process design to choose as all designs are affected in a similar manner. It is also worth noticing that the most relevant parameters are not necessarily the parameters that have a large influence on the sensitivity matrix $\boldsymbol{Q}$, because for the calculation of $\boldsymbol{Q}$, only individual lab experiments for one unit are considered, while for the determination of the influencing parameters, the overall process is considered. Kaiser et al. [40] therefore extended the previous approach [29] by the inclusion of the sensitivity of the cost function that is used in the model-based design optimization in the selection and weighting of the parameters in mb-DoE.

The set of parameters that are considered for the mb-ODoE is reduced here to the most influencing parameters. Which parameters have the largest influence on the discrete design decisions is determined by the computation of the partial dependence which is explained in section 2.3. Additional experiments are used to estimate all model parameters to reduce the parametric uncertainties. The improved estimation of all parameters leads to a more accurate prediction of the process cost and comes with no additional effort.

2.3. Identification of the influencing parameters

Identifying the parameters that influence the design decisions most is crucial for efficient and effective experiment-based development strategies. We use linear discriminant analysis (LDA) [41] to calculate the feature importance and to determine these key parameters. LDA is combined with partial dependence analysis to provide a comprehensive characterization of the impact of the parameters on the optimal discrete design decisions.

The starting point of the methodology is to categorize the optimization results into distinct classes, each representing an optimal discrete design decision. LDA, a statistical method that is traditionally used for dimensionality reduction and classification, is employed to separate these classes. LDA works by finding linear combinations of features that best separate the different classes, maximizing the ratio of between-class variance to within-class variance.

Central to this analysis is the discrimination function, which describes the distance between a point x, in this case one realization of uncertain parameters, and the average μ_l of the uncertain parameters of a given class of designs divided by the variance σ^2 of the uncertain parameters. For a point x and a class l, the discrimination function $d_l(x)$ is defined as [42]:

$$d_l(x) = -\frac{||x-\mu_l||}{2\sigma^2}. \tag{4}$$

The discrimination function provides a decision boundary in the parameter space, thus enabling the classification of new data points based on their proximity to the class centers.

To quantify the impact of the uncertain parameters on the classification and, by extension, on the optimal design alternative, we employ partial dependence analysis. This technique provides insight into the effect of a given parameter on the predicted outcome of a machine learning model, in this case, the optimal design class. The partial dependence function $f^s(x^s)$ for a parameter s is mathematically expressed as [43]:

$$f^s(x^s) = E_c[f(x^s, X^c)] = \int f(x^s, X^c) p_c(X^c) dX^c \tag{5}$$

In this equation, x^s represents the value of the parameter s, X^c represents all other parameters, and $p_c(X^c)$ denotes the probability distribution of X^c. The partial dependence is computed by varying the value of a single parameter while keeping all others constant. This process is averaged over the set of all classified realizations of the samples.

The partial dependence is a measure of parameter importance, showing how changes in a specific parameter affect the model predictions across the parameter space. Parameters demonstrating a significant effect on the discrimination function, and consequently on the optimal design, are identified as key influencers in the decision process.

In the subsequent mb-ODoE, only the parameters that show a significant effect on the structural decisions are included. This focused approach not only enhances the efficiency of the optimization within the mb-ODoE but also improves the interpretability of the results, as the relationships between key parameters and optimal designs become more apparent.

3. The hydroaminomethylation process and its model

Hydroaminomethylation is used to produce long chain amines for the production of e.g. surfactants. The homogeneously catalyzed hydroaminomethylation is characterized by mild reaction conditions and hence is a safe and less energy intensive alternative to a heterogeneously catalyzed reaction. Here we consider the hydroaminomethylation of 1-decene which can be performed using a rhodium catalyst, leading to high yields and selectivities [44]. The reaction scheme is shown in Fig. 2. The reaction consists of two subsequent reaction steps. The first step is a hydrofomylation of decene to undecanal, which reacts in a second step with diethylamine in a reductive amination by a condensation and hydration. In the condensation reaction, water is formed as a byproduct.

As rhodium is expensive, efficient recycling of the catalyst is one of the main objectives for the process design. Thermomorphic multiphase systems (TMS) are an effective means for recycling homogeneous catalysts [45]. These systems consist of reactants and solvents that are selected such that they form a homogeneous mixture at reaction temperature and split into two phases at a lower temperature. One of these phases is supposed to be the catalyst rich phase, which is recycled back to the reactor, and the other phase is the product rich phase that is further passed to a downstream process. Originally for this reaction three solvents were used to achieve the phase switching behavior [46], but later research focused on systems that consist of only two solvents [47]. Bianga et al. [44] demonstrated that the hydroaminomethylation of 1-decene can be performed in a TMS with methanol and dodecane as solvents. In this system, the catalyst dissolves in the polar methanol phase and can be recycled while the product stays in the nonpolar dodecane phase.

A simplified flowsheet of the HAM process that was used in the mini plant demonstration described in Schlüter et al. [48] is shown in Fig. 3. For the implementation of the TMS system a heat exchanger and a decanter are applied for cooling and phase separation after the reaction. The feasibility of this process design was successfully demonstrated with high conversion of the feed streams. The reaction was performed at 125 °C and 36 bar, the separation in the decanter was performed at 5 °C and 36 bar and the AMS NanoPro S-3012 was used and operated at 36 bar. The flowsheet contains the decision to use a thermomorphic multiphase system or to feed dodecane only after the reactor as an extraction agent.

3.1. Reactor and decanter model

The reactor is modeled by material balances for all components and the kinetic model from Kortuz et al. [49]. As thermodynamic models, surrogate models that were trained on sampled data of the solution of the equation of state by PC-SAFT [50] are used both for the reactor model and for the decanter model. Classifiers that were also trained on PC-SAFT data are used as constraints to ensure a single phase mixture in the reactor and a two-phase separation in the decanter. Details about surrogate models for thermodynamic models in process optimization

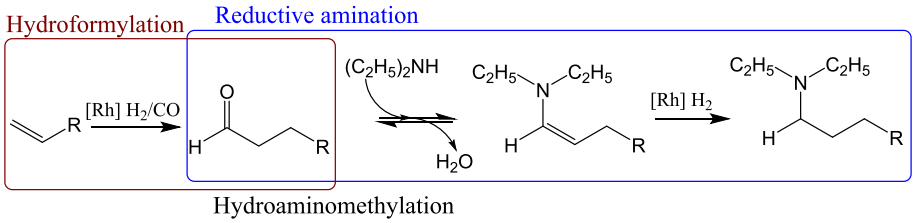

Fig. 2. Reaction scheme of the hydroaminomethylation taken from [29]. The reaction consists of two consecutive reaction steps, hydroformylation and reductive amination.

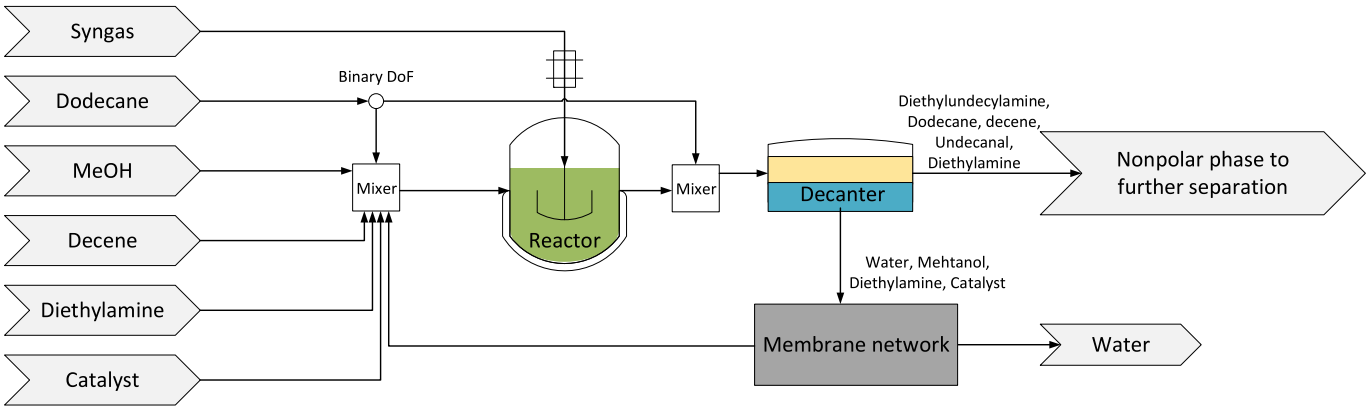

Fig. 3. Flowsheet of the hydroaminomethylation process, including the decision to use a TMS system or to add dodecane as an extraction agent adapted from [29].

can be found in the work of Nentwich and Engell [51] and about the specific model in the work of Kaiser and Engell [29].

3.2. Membrane model

Models for membrane processes can be established at different scales such as local flux models, module models and process models [22]. Due to the larger uncertainties in early design stages, we focus on local flux models to describe the separation performance of the membrane combined with simplified process models to describe multi-stage arrangements.

There is a large variety of local flux models available in literature which differ slightly in their assumptions and simplifications with different trade-offs between model complexity and accuracy [52]. To describe the local flux of each component present in the reaction mixture a solution-diffusion type model is applied in this work. We used a flux model which is similar to that developed by Fierro et al. [53], because it incorporates the non-ideality of the liquid phase, while still only requiring a single membrane specific model parameter for each component. The local flux for each component is described by eq. (6).

$$J_i = P_i \cdot \left(\ln(a_{i,F}) - \left(\ln(a_{i,P}) - \frac{v_i \cdot \Delta p}{R \cdot T} \right) \right) \tag{6}$$

Here J_i is the molar flux of component i, Pi the permeance of component I, $a_{i,F}$ and $a_{i,P}$ are the activity of component I in the feed and in the permeate, v_i is the molar volume of component i, Δp the pressure difference from feed to permeate side and R and T are the ideal gas constant and temperature.

This model uses the activity of each component on the feed and permeate side of the membrane to establish its driving force across the membrane. Thus, in order to calculate the total permeate flux as the sum of the individual fluxes, the activity of each component in the mixture is required. The activities are defined as the product of the molar fraction x_i and the activity coefficient γ_i:

$$a_i = x_i \bullet \gamma_i. \tag{7}$$

The activity coefficients are calculated using the fugacity coefficient of component i in the mixture φ_i and of the pure component $\varphi_{i,0}$ at the same temperature and pressure:

$$\gamma_i = \frac{\varphi_i}{\varphi_{i,0}}. \tag{8}$$

The fugacity coefficients can be calculated by an equation of state. Since PC-SAFT [50] is known as an accurate equation of state and all required parameters of the involved components are available in literature [54], it is the method of choice in this work. However, as PC-SAFT performs internal iterations to solve the system of equations, this leads to high computation times and is not suitable for gradient-based optimizations with many scenarios. Therefore, we compute the fugacity coefficients by the same surrogate models as are used for the description of the phase equilibrium in the reactor and the decanter [51]. These models were trained for the specific operating range as described in Kaiser and Engell [29].

3.3. Membrane superstructure

In the hydroaminomethylation process, water is formed during the reductive amination reaction and leaves the decanter in the polar phase, which is recycled back to the reactor. Therefore, the produced water must be separated from the recycle stream to prevent an accumulation in the reactor, which would otherwise decrease the reaction performance due to the formation of a biphasic system in the reactor [44]. Furthermore, with an increasing amount of water, the volume of the polar phase would increase over time, leading to a biphasic outlet from the decanter and thus a significant loss of the catalyst. A sufficiently hydrophilic membrane that also provides a low molecular cut-off can be used to achieve the removal of water and to improve the retention of the catalyst at the same time, thus improving the economics of the process, as it was presented in previous work [48]. For such a membrane separation suitable structure and membranes have to be selected. These decisions are included in the superstructure that is shown in Fig. 4. The flowsheet presented in Fig. 3 also includes the structural decision whether the reaction is performed in a TMS or the nonpolar solvent dodecane is only added after the reaction as an extraction agent. Two different membranes have been found suitable in pre-screening studies. The superstructure optimization aims at finding an optimal interconnection with up to three stages and selecting the best membrane for each stage. The permeate and the retentate stream can be further purified by additional membranes. The first stage of the membrane network must always be present, the further stages are optional, either one additional membrane, two or none can be used.

4. Materials and methods

For modelling of the performance of the membranes, experiments are required to estimate model parameters for the local flux model (6). A simplified mixture of the most relevant components in the membrane separation was used in the model. These components are listed in Table 1, with a short description of their relevance.

4.1. Membranes and chemicals

The chemicals used in this work are identical to those described in previous work [44,48]. The two membranes that were compared are the AMS NanoPro S-3012 (NP3012) and AMS NanoPro S-3014 (NP3014) membranes both manufactured by AMS technologies (now UNISOL

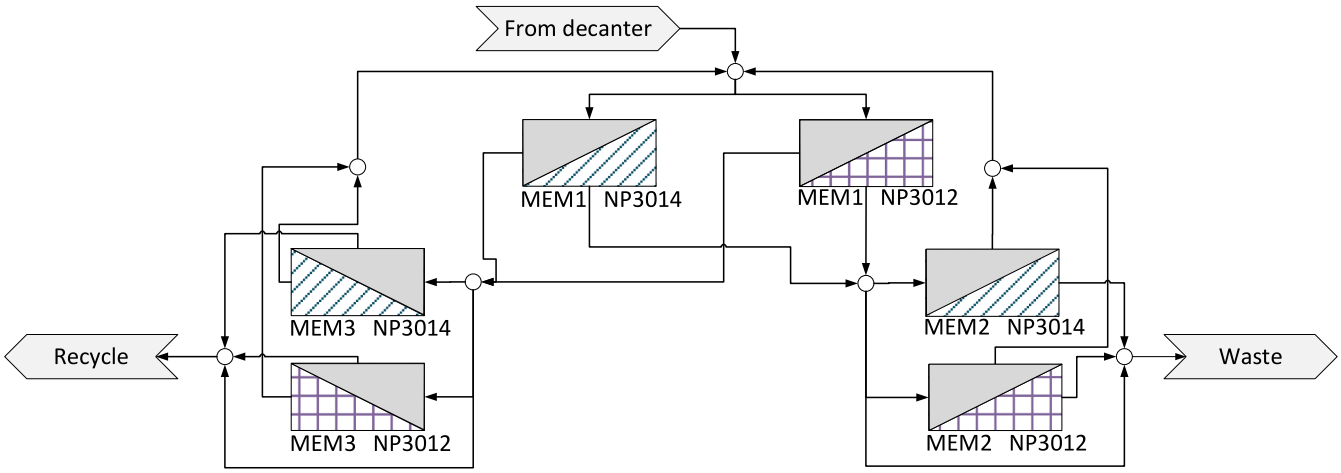

Fig. 4. Superstructure representation of the membrane network. In the first stage (MEM1) either material NP3012 (squared) or NP3014 (striped) can be used. Then the retentate can be filtered optionally by either material (MEM3) and the permeate can be optionally filtered by either material (MEM2).

Table 1
Components considered for the membrane model.

Component	Description
Methanol	Polar solvent forming the TMS
n-Dodecane	Non-polar solvent forming the TMS
Diethylamine	Substrate for the hydroaminomethylation reaction. The second substrate 1-decene, was not considered, as it is mainly present in the non-polar phase.
Water	Co-product of the hydroaminomethylation reaction
Diethylundecylamine (DEUA)	Product of the hydroaminomethylation reaction
Sulfoxantphos (Ligand)	Ligand of the catalyst species for the hydroaminomethylation. The catalyst complex is only present under reaction conditions, therefore the retention of the ligand is used to estimate the loss of catalyst.

membrane technology). The selection was based on the results of previous membrane screening experiments for the same application [48]. The two membranes differ mainly in their molecular weight cutoff (MWCO) and their expected flux. The MWCO is given as 200 g mol^{-1} for the NP3012 and as 400 g mol^{-1} for the NP3014 [55,56]. As is common in membrane separations, the lower MWCO of the NP3012 comes with the trade-off of lower membrane permeance. The described methodology can also be applied using further types of membranes with other properties, however based on previous tests [48] the AMS membranes showed the best performance and stability so that only the two membrane types NP3012 and NP3014 were included here.

4.2. Membrane experiments

The membrane experiments were performed in a lab-scale set-up similar to that described by Schlüter et al. [48], which comprises a feed tank at ambient pressure, an HPLC pump for pressure generation, a circulation pump, a heat exchanger and three membrane modules connected in series. Before every experiment, three membranes cutouts of the same membrane were placed in the cells and the feed solution was filled into the feed tank. No other pretreatment steps of the membrane were performed. Then the experiment was started using the two pumps, temperature and pressure were set according to the required conditions. After reaching the required temperature and pressure, the experiment was conducted for at least four hours until constant permeate flux was achieved, which was monitored by Coriolis flow meters in the permeate lines. During the experiments the retentate and the permeate were both recycled to the feed tank. At the end of the experiment, permeate and feed samples were taken and analyzed by gas chromatography (GC), HPLC analysis and Karl-Fischer titration to determine the mass fractions of all components (HPLC for the mass fraction of the ligand, Karl-Fischer titration for the mass fraction of water and GC measurements for the mass fraction of all remaining components). Details about the analytics can be found in the work of Schlüter et al. [44,48].

The membrane performance is characterized by the total permeate flux (eq. (9)) and component specific rejections as defined by eq. (10):

$$J = \frac{\dot{m}}{A} \tag{9}$$

$$R_i = 1 - \frac{w_{i,Permeate}}{w_{i,Feed}} \tag{10}$$

In eq. (9), J is the total flux, $\dot{m}$ the measured mass flow and A the membrane area of each cell. In eq. 10, R_i is the rejection of each component and $w_{i,Permeate}$ and $w_{i,Feed}$ the mass fractions of each component in the feed and permeate stream respectively.

Note that in some experiments, one of the membrane cutouts showed significantly different results compared to the other two membranes. In these cases, the respective cutouts were treated as outliers and not used for parameter regression and further modelling. This is also indicated in the description in the supporting information.

5. Superstructure optimization for the hydroaminomethylation of 1-decene

The process is modeled as described in Section 4 and considered as a set of equality constraints for the optimization. The total annualized production cost (CPT) is used as the objective function for the process optimization. The CPT is computed as

$$CPT = \frac{C_{op} + \frac{C_{invest}}{10}}{\dot{m}_{DEAU}} \tag{11}$$

The cost consists of the operational cost, including the raw materials, utilities and the exchange of the membrane modules every two years as has been considered in other work [57], and the investment cost with a depreciation of 10 years. The cost are optimized for a fixed annual capacity of the plant of 10 kt of diethyl undecylamine.

As described in Section 2.1, the various degrees of freedom of the design and of the operation of the process are treated differently. The design DoFs are optimized in the first stage, i.e. they are the same for all scenarios, and the operational DoF are optimized in the second stage, i.e. it is assumed that they can be adapted optimally to the real behavior of the process during operation, by feedback control, real-time

optimization [30–32] or manual adaptation by the operators. The different DoFs and their lower and upper bounds are shown in Table 2.

For the design of the membrane network, the accuracy of the solution-diffusion model is crucial. Therefore, the permeances P_i of all components are considered as uncertain parameters. The prediction of the activity coefficients is assumed to be possible with comparatively small errors because the surrogate models represent the PC-SAFT data accurately and PC-SAFT was shown to provide accurate predictions for the system considered here [50]. The loss of catalyst has a strong influence on the operating cost and this cost depends on the current price of the catalyst. As the rhodium price largely varies, it is also considered as an uncertain parameter in the superstructure optimization under uncertainties. Since this work focuses on the design of the membrane network only, other parameters (e.g. uncertainties in the kinetic model) are not considered here, they were addressed in previous work [29].

6. Results

6.1. Membrane experiments

In total five experiments (E1-E5) were conducted in the course of this work. The procedure for the experiments was as detailed in Section 4.2. The first two experiments, E1 and E2 were used to establish a first membrane model for the two candidate membranes (NP3012 & NP3014). The experiments E3-E5 were used to refine the model of the NP3012 membrane, and the experimental conditions were determined as the solution of a single ODoE, for which the temperatures, pressures and mass fractions of the components of each of the three experiments were determined, subject to the constraint that the mass fractions were constrained to be the same for all three experiments to allow for the use of only one mixture enabling a comparably fast adaptation of the operating conditions of the experiments.

Table 2
Degrees of freedom used in the superstructure optimization and their bounds.

Description	Type	Variable	Unit	Min	Max
Membrane type stage 1	Binary design DoF	MEM1	–	0	1
Membrane type stage 2	Binary design DoF	MEM2	–	0	1
Membrane type stage 3	Binary design DoF	MEM3	–	0	1
Stage 2 active	Binary design DoF		–	0	1
Stage 3 active	Binary design DoF		–	0	1
TMS is used	Binary design DoF	TMS	–	0	1
Area stage 1	Continuous design DoF	A_1	m^2	0.1	10
Area stage 2	Continuous design DoF	A_2	m^2	0.1	10
Area stage 3	Continuous design DoF	A_3	m^2	0.1	10
Reaction temperature	Recourse variable	T_R	K	373.15	398.15
Carbon monoxide partial pressure	Recourse variable	p_{CO}	bar	5	15
Hydrogen partial pressure	Recourse variable	p_{H_2}	bar	20	35
Decanter and membrane operating temperature	Recourse variable	T_D	K	273.15	298.15
Solvent ratio	Recourse variable	$\frac{w_{MeOH}}{w_{DDC}}$	$[-]$	1	10
Catalyst to decene ratio	Recourse variable	$\frac{w_{cat}}{w_{decene}}$	$[-]$	$1e^{-4}$	$5e^{-4}$

6.1.1. Experiments E1 & E2

With the goal to determine a first set of parameters that can be used in the process optimization under uncertainty, one experiment per membrane candidate was performed at 40 bar feed pressure and a temperature of 28C. These were chosen based on previously used operating conditions [48] and are inside the range of the optimization of both variables. The feed concentrations for the experiments are summarized in Table S1 in the supporting information. The resulting performance data for the initial experiments E1 and E2 are depicted in Fig. 5a and b as total flux and rejection for the individual components plotted against the feed pressure. Additionally, the permeances for each component were determined using least squares regression. The predicted performance data is also depicted in Fig. 5 as solid lines. The values of the permeances and their confidence intervals are presented for both membrane types in the supporting information in Table S2 together with parity plots for the partial fluxes of each component (Figs. S1 and S2).

The model predictions match the measured data with good agreement. This is not surprising because the same set of pressure, temperature and composition parameters was used for parameter estimation so that the uncertainty at these conditions results only from the different membrane samples that were tested. This is also visible from the small error bars. The solution-diffusion model seems to work well for these membranes.

The measured fluxes and rejections are also in good agreement with previous work using the NP3012 membrane and a similar mixture of components [19,48]. Scharzec et al. [19] measured membrane fluxes in the range of 4 kg m^{-2} h^{-1} with a test mixture consisting of methanol, water and a catalyst ligand at 20 bar feed pressure. Assuming a linear pressure-flux relation, 8 kg m^{-2} h^{-1} would be expected at 40 bar. Schlüter et al. [48] used more complex model solutions and catalyst solutions from miniplant experiments and achieved membrane fluxes between 0.5 and 8.7 kg m^{-2} h^{-1} at 36 bar feed pressure. There also very similar rejections were measured for all components that were used in this work.

6.2. Superstructure optimization I

Using the permeance values that were initially determined from experiments E1 and E2, a superstructure optimization under uncertainties was performed to determine the optimal membrane network. 40 discrete scenarios of process and cost function parameters were defined by a Latin hypercube sampling within the 95 % confidence interval. The results of the superstructure optimization can be seen in Fig. 6. The figure shows the predicted cost for the 9 best structurally different design alternatives. Each line represents one discrete scenario of the uncertain parameters. The dots represent the optimal design for each scenario. Design 1 gives the lowest predicted cost for most scenarios. However, for some scenarios, design 2 or design 4 lead to lower costs.

Since all other designs show higher cost values for all scenarios, they can already be discarded after the first iteration of the design process and the remaining investigations can focus on design 1, 2 and 4. A description of the different designs is presented in Table 3. The chosen membrane material is indicated if the corresponding membrane stage is used.

An analysis of the design alternatives gives deeper information about the structural decisions that are crucial for the expected production cost. First, generally a TMS process, i.e. feeding dodecane into the reactor and not only to the decanter is not advantageous. Second, out of the 9 best designs, 5 use a two-stage membrane process while the remaining 4 designs use a single stage membrane separation. Comparing the results between the best single stage process (design 3) and the designs 1, 2 and 4, which are all two-stage processes, it can be seen that a two-stage process leads to lower total production cost. While in the designs 4, 5, 6 and 8 membrane type 1 is used for the first stage of the membrane

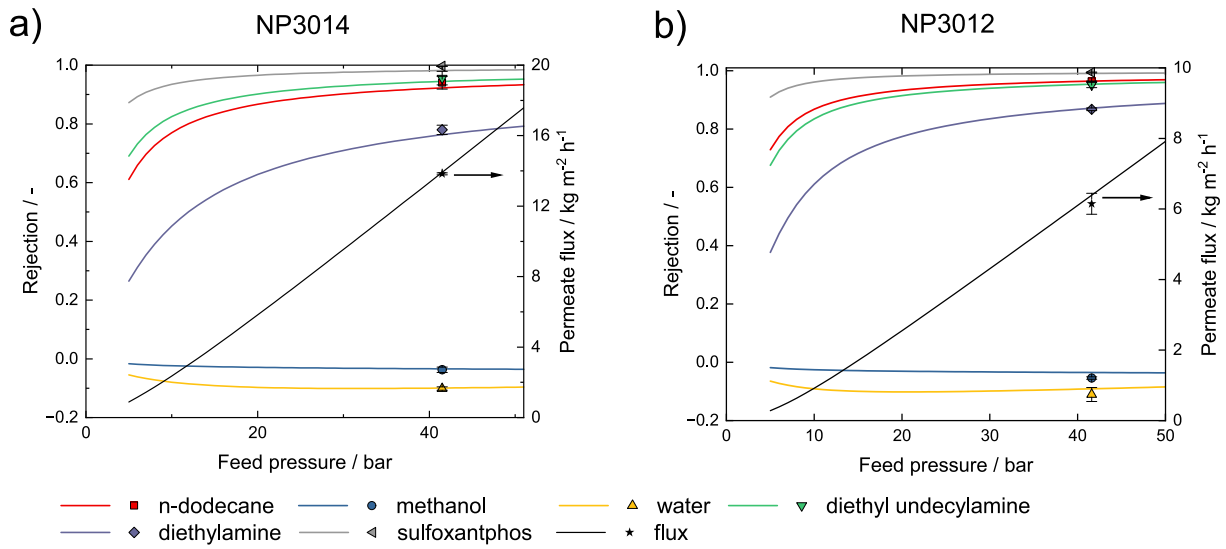

Fig. 5. Experimental results (symbols) and model predictions (lines) after E1 (a) and E2 (b). The data points (symbols) are average values and the error bars indicate the standard deviations, both estimated from the measured values for the three membrane samples used in each experiment.

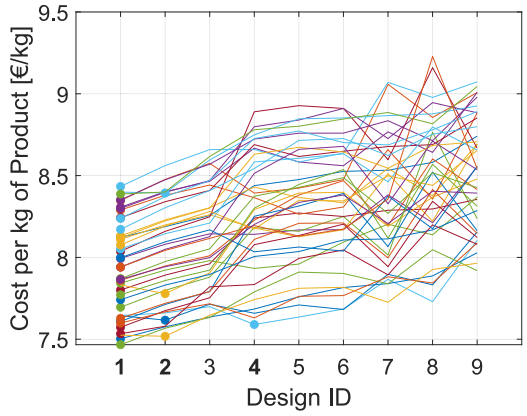

Fig. 6. Results of the superstructure optimization after the first iteration. Each line represents one realization of the uncertain parameters. The dots show which design has the lowest cost for each scenario. It can be seen that only designs 1, 2 and 4 show the lowest cost for any of the uncertain scenarios.

network, in all other designs membrane type 2 is used for the first stage. Designs 2 and 4 only differ in the choice of the membrane material of the first stage but show significant differences in the production cost. Thus, it can be concluded from the first superstructure optimization that the decision on a membrane type for the first stage of the network is essential. Therefore, in the next step designs 1 and 2 are lumped into one design category and the goal of the identification of the crucial parameters is to identify the parameters that need to be determined more precisely to decide between the combined design 1 and 2 and design 4, i.e. on the membrane which should be used in the first state. Further refinement to decide between designs 1 and 2 can be done later if necessary.

To identify the parameters that are leading to different optimal structures, the partial dependences were computed. The partial dependence plot is presented in Fig. 7.

For the different designs, the score of the partial dependence is plotted over the scaled value of the uncertain parameters. The variation of the score over the scaled uncertain parameter represents the influence of the parameter on the discrete design decision. It can be seen from Fig. 7 that only the permeance of methanol for the NP3012 membrane influences the design decision, because it is the only parameter for which the class with the highest score changes. Although the price of the catalyst has a high impact on the overall production cost it does not influence the decision on the optimal design.

To validate the outcome of the partial dependences, a superstructure optimization under uncertainty was performed without considering the uncertainty in the permeance of methanol for NP3012 while all other uncertainties were the same as for the previous superstructure optimization. In Fig. 8, it can be seen that without this uncertainty design 1 is optimal for all realizations of the uncertain parameters. The decision between design 1 and 2 in this case is independent of the remaining uncertainties, i.e. if the permeance of methanol for membrane type 1 is exactly known no further experimental investigations are necessary.

6.3. *Optimal design of experiments and experimental results*

As a conclusion from the analysis of the partial dependencies, new experiments were planned using an mb-ODoE that is focused on determining the methanol permeance of membrane NP3012 only. Since a large fraction of the workload during the experiments results from the preparation of the mixture as well as filling and cleaning work, 3 consecutive experiments (E3 – E5) were planned that are restricted to have the same composition, so that they can be run without changing the feed solution or the membrane. This reduces lab work significantly and gives a good trade-off between required lab work and computational

Table 3
Description of the design IDs. The membrane material is given for each stage of the network (only if the stage is usen in the specific design). It is further given if a TMS system is used or if one solvent is added after the reaction.

ID	1	2	3	4	5	6	7	8	9
MEM1	NP3012	NP3012	NP3012	NP3014	NP3014	NP3014	NP3012	NP3014	NP3012
MEM2	–	–	–	–	–	NP3014	–	–	–
MEM3	NP3012	NP3014	–	NP3014	–	–	–	–	NP3012
TMS?	no	no	no	no	no	no	yes	yes	yes

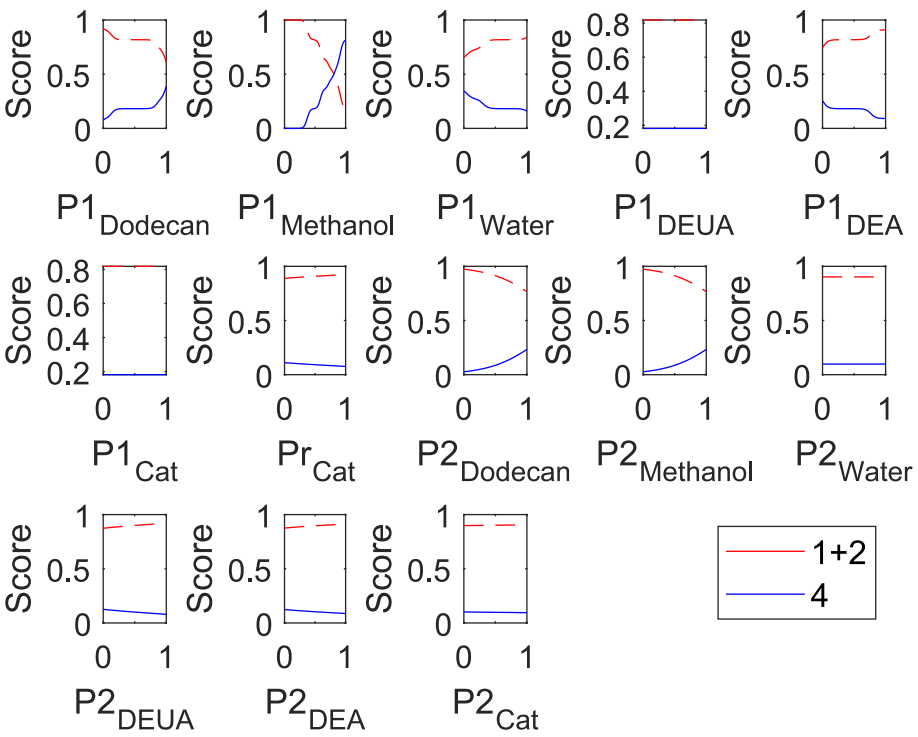

Fig. 7. Partial dependence plot after the first iteration. P1 corresponds to the permeances of NP3012 and P2 to the permeances of NP3014. $P2_{Cat}$ is the price of the rhodium catalyst.

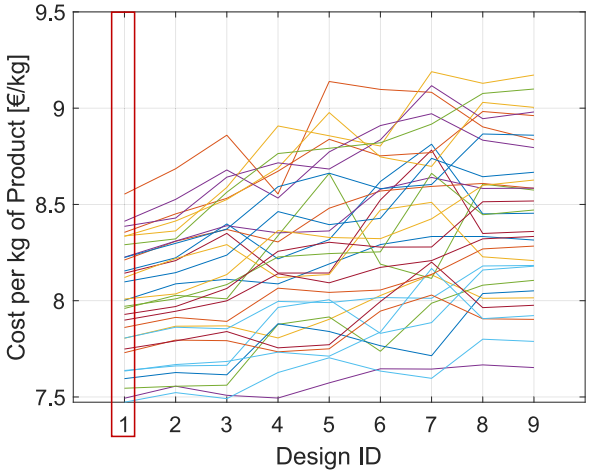

Fig. 8. Results of the superstructure optimization using the ranges of the uncertain parameters after the initial parameter estimation, except for the permeance of methanol for membrane NP3012 which is assumed to be exactly known. For each uncertain scenario the minimum costs result for design 1 which is indicated by the red box.

effort. In addition to the concentration, temperature and pressure of the experiments were optimized. The results of the ODoE are shown in the supporting information in table S3.

The experiments E3 to E5 for the membrane NP3012 were performed consecutively using the feed concentrations, pressures, and temperatures shown in Table S1. The same procedure as for the experiments E1 and E2 was used. Based on the experimental data all model parameters were updated employing the full set of experimental data (E2-E5). The model predictions for each experiment E2 to E5 are compared to the experimental data in Fig. 9 as a parity plot for the partial fluxes for each component. In general, the model predictions are in good agreement with the experimental data for most of the components. Some deviations are visible for the ligand sulfoxantphos, where the predicted partial fluxes are slightly higher than the experimentally measured ones, which does however result in an overestimation of the ligand loss in the permeate, which results in a rather conservative cost estimation.

The resulting model parameters are listed in the supporting information together with their 95 % confidence intervals. Comparing the data from the first experiment for this membrane and the overall set reveals that the uncertainty of the methanol permeance was decreased significantly. On the other hand, some of the other permeances show a

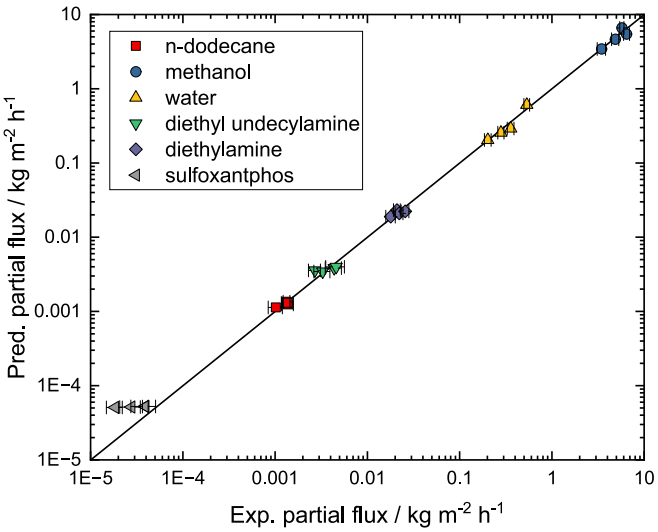

Fig. 9. Parity plot of partial fluxes for the NP3012 based on experiments E2-E5. Model predictions for each experiment were made for the averaged values obtained from the three different membrane samples that were used in the experiment. Error bars represent the standard deviation of the experimental fluxes calculated based on the measured values for the three membrane samples in each experiment.

higher uncertainty when the parameters are estimated from all experiments compared to only the first experiment. This can be explained because the uncertainty of the permeance in a single experiment only originates from different membrane samples (i.e. physically different cut-outs from a larger sheet), whereas the total uncertainty from several different experiments also includes the uncertainty originating from different set points of the pressure, temperature and composition. Thus, the estimated permeances, especially for the components with small mass fractions in the feed, show higher uncertainties when estimated from all experiments.

With the updated parameters and their ranges of uncertainty, the superstructure optimization was then repeated to determine whether a single variant would result as the optimal design.

6.4. *Superstructure optimization II*

After performing the designed experiments and updating the parameters of the permeances, the superstructure optimization under uncertainties was repeated. New scenarios were determined by Latin hypercube sampling within the updated 95 % confidence interval. Since the other designs could already be discarded, only designs 1, 2 and 4 were considered. The results of the final superstructure optimization are shown in Fig. 10. It can be seen that due to the smaller uncertainty in the permeance of methanol, design 4 which corresponds to the design using NP3014 in the first stage of the membrane network, can now also be discarded. The decision on NP3012 is now clearly advantageous. Although either design 1 or 2 are optimal for different scenarios, the differences between the predicted costs are small (maximum 0.05 €/kg) and the selection of either of the designs can be justified, e.g. based availability of the membranes or on the argument that using only one type of membranes would be preferable. It should be mentioned that the work refers to an early stage of process design where the accuracy of the predicted cost is way larger than the differences between these two designs. The structures of design 1 and 2 are depicted in Fig. 11. As design 1 shows the lowest production costs for most of the uncertain scenarios, it is considered the best choice for the final process design. It consists of two membrane stages both with the material NP3012. The polar phase that is separated in the decanter contains mostly water and methanol, a large amount of the unreacted diethylamine, traces of the other components and the catalyst as it is dissolved in water, is passed through the first membrane stage. Here the retentate that contains most of the catalyst, methanol, some of the water, and the other nonpolar components is fed back to the reactor as a recycle stream. A second membrane stage is used to filter the permeate to recycle the catalyst that is contained in the permeate. The waste stream contains mainly water. With this structure not only the loss of methanol, but most importantly the loss of the expensive catalyst is reduced.

Since the experiments E3-E5 were only performed for one composition, attention should be paid that this composition is not too far away from the optimal operating points resulting from the superstructure optimization. It is seen from the optimal operating ranges shown in Table S4 that the experimental concentration and the optimized process concentration of the most important component methanol match very well.

7. Summary

While several examples can be found in the literature where superstructure optimization is used for the design of membrane networks, these networks are usually optimized separately from the other elements of the process. In this work, we presented a methodology to apply model-based design optimization to an entire process that includes a membrane network. The methodology is based on two-stage optimization under uncertainties where the structural design decisions (choice and sizing of unit operations and interconnection structures) are optimized for all scenarios of uncertain parameters under the assumption that the operational parameters are optimized for each scenario during operation when the uncertainty materializes. The approach was applied to the design of a membrane network for the hydroaminomethylation of 1-decene in a multi-phase system, a process with a large number of relevant components, a complex reaction network, and complex thermodynamic equilibria. Several stages and two different membrane materials were considered in the superstructure optimization of the membrane section.

By this approach, the interaction between the design of the membrane process and of the other process units is taken care of. Since membrane separation models usually need to be fitted to dedicated experiments and the resulting models usually are prone to significant uncertainties, these uncertainties are considered in the superstructure optimization. We used the information from the superstructure optimization to discard many process alternatives already in the first stage of the design process. To choose between the remaining competing best design alternatives, a model refinement was performed based on experiments that were planned using model-based optimal design of experiments. These experiments focus on determining those model parameters that are most relevant for the structural design decisions to reduce the experimental effort.

We could show that by using the presented methodology only one set

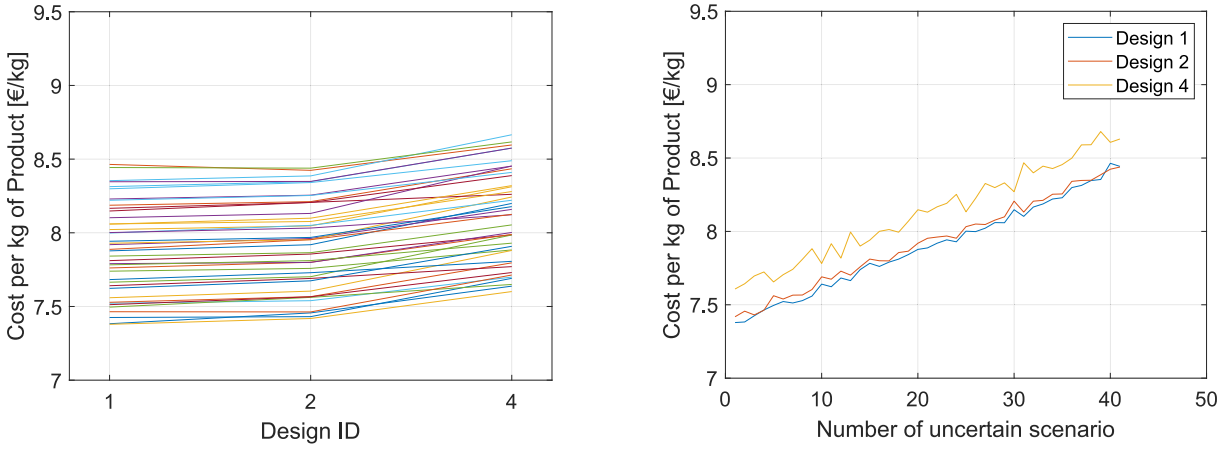

Fig. 10. Results of the superstructure optimization after the second iteration. In plot on the left hand side, the costs are presented for the designs that we identified to be potentially optimal before. As in the figures above, each line represents one realization of uncertain parameters. Additionally, on the right hand side the costs are plotted for the three best designs over the uncertain scenarios. It can be seen that the costs for design 4 are higher than for design 1 and 2 for all uncertain scenarios while the costs of design 1 and design 2 do not differ significantly.

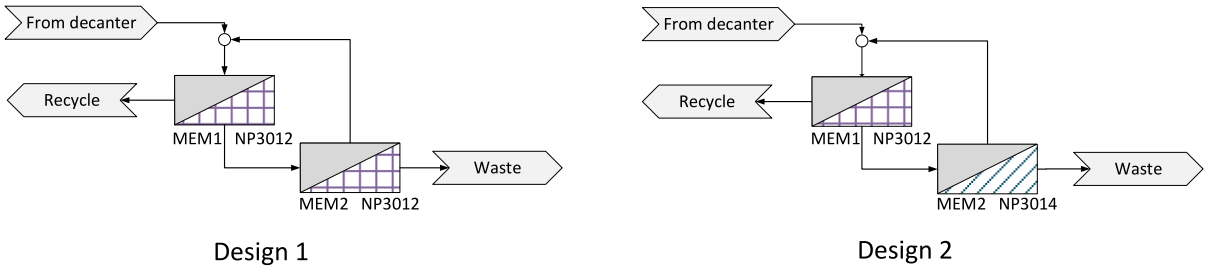

Fig. 11. Structures of the optimal designs 1 and 2. The designs only differ in the membrane material of the second stage.

of laboratory experiments in addition to first screening experiments was necessary to determine a membrane model that is accurate enough to make a decision about the membrane material and the membrane network of the optimal process configuration. A validation of the process performance afterwards needs to be done in investigations of the full set-up, e.g. in a miniplant as in [48,58].

The work can and should be extended in several dimensions, using more detailed membrane models, including more uncertainties simultaneously, and optimizing larger flowsheets with larger models of the units, e.g. distillations columns. This requires further work on the stability and efficiency of the numerical solution strategy for the superstructure optimization under uncertainty which provides the basis of such investigations. It should be mentioned that, similar to the work in [29] this paper is based on a divide-and-conquer approach were experiments to obtain models of different process elements are optimized separately. Indeed, these experiments are independent, but potentially coupled by the chosen operating conditions. We validated this choice here ex post. A full simultaneous design would certainly be of interest, but if the systematic approach proposed here for individual process elements will be adopted industrially it would already lead to significant benefits, as demonstrated.

CRediT authorship contribution statement

Stefanie Kaiser: Writing – original draft, Visualization, Validation, Methodology, Investigation, Conceptualization. **Stefan Schlüter:** Writing – original draft, Visualization, Validation, Methodology, Investigation, Conceptualization. **Mirko Skiborowski:** Writing – review & editing, Supervision, Funding acquisition. **Sebastian Engell:** Writing – review & editing, Supervision, Funding acquisition.

Declaration of competing interest

The authors declare that they have no known competing financial interests or personal relationships that could have appeared to influence the work reported in this paper.

Acknowledgements

Funded by the Deutsche Forschungsgemeinschaft (DFG, German Research Foundation) - TRR 63 “Integrated Chemical Processes in Liquid Multiphase Systems” (subprojects D1 and D3) - 56091768. Gefördert durch die Deutsche Forschungsgemeinschaft (DFG) - TRR 63 “Integrierte chemische Prozesse in flüssigen Mehrphasensystemen” (Teilprojekte D1 und D3) - 56091768.

Appendix A. Supplementary data

Supplementary data to this article can be found online at https://doi.org/10.1016/j.cej.2025.170385.

Data availability

Data will be made available on request.

References

[1] L.T. Biegler, Grossmann, Ignacio E. Westenberg, Arthur W., Systematic Methods of Chemical Process Design, first ed., Prentice Hall, 1997.
[2] S.D. Barnicki, J.R. Fair, Separation system synthesis: a knowledge-based approach. 1. Liquid mixture separations, Ind. Eng. Chem. Res. 29 (1990) 421–432, https://doi.org/10.1021/ie00099a018.
[3] G. Schembecker, K.H. Simmrock, Heuristic-numeric design of separation processes for azeotropic mixtures, Comput. Chem. Eng. 21 (1997) S231–S236, https://doi.org/10.1016/S0098-1354(97)87507-2.
[4] J.M. Douglas, A hierarchical decision procedure for process synthesis, AICHE J. 31 (1985) 353–362, https://doi.org/10.1002/aic.690310302.
[5] M. Urselmann, S. Barkmann, G. Sand, S. Engell, Optimization-based design of reactive distillation columns using a memetic algorithm, Comput. Chem. Eng. 35 (2011) 787–805, https://doi.org/10.1016/J.COMPCHEMENG.2011.01.038.
[6] T. Janus, C. Foussette, M. Urselmann, S. Tlatlik, A. Gottschalk, M. Emmerich, T. Bäck, S. Engell, Optimization-Based Process Synthesis Based on a Commercial Flowsheet Simulator, Chemie-Ingenieur-Technik 89 (2017) 655–664, https://doi.org/10.1002/cite.201600179.
[7] L. Mencarelli, Q. Chen, A. Pagot, I.E. Grossmann, A review on superstructure optimization approaches in process system engineering, Comput. Chem. Eng. 136 (2020) 106808, https://doi.org/10.1016/j.compchemeng.2020.106808.
[8] M. Skiborowski, Synthesis and design methods for energy-efficient distillation processes, Curr. Opin. Chem. Eng. 42 (2023) 100985, https://doi.org/10.1016/j.coche.2023.100985.
[9] M. Skiborowski, M. Rautenberg, W. Marquardt, A novel approach to hybrid evolutionary-deterministic optimization in process design, Computer Aided Chemical Engineering 32 (2013) 961–966. doi:https://doi.org/10.1016/B978-0-444-63234-0.50161-5.
[10] K.F. Kruber, T. Grueters, M. Skiborowski, Advanced hybrid optimization methods for the design of complex separation processes, Comput. Chem. Eng. 147 (2021) 107257, https://doi.org/10.1016/j.compchemeng.2021.107257.
[11] S. Liu, H. Li, B. Kruber, M. Skiborowski, X. Gao, Process intensification by integration of distillation and vapor permeation or pervaporation - An academic and industrial perspective, Results in Engineering 15 (2022) 100527, https://doi.org/10.1016/j.rineng.2022.100527.
[12] I.E. Grossmann, R.W. Sargent, Optimum design of chemical plants with uncertain parameters, AIChE Journal 24 (1978) 1021–1028, https://doi.org/10.1002/aic.690240612.
[13] G.E. Paules IV, C.A. Floudas, Stochastic programming in process synthesis: A two-stage model with MINLP recourse for multiperiod heat-integrated distillation sequences, Comput. Chem. Eng. 16 (1992) 189–210, https://doi.org/10.1016/0098-1354(92)85006-T.
[14] Z.N. Pintarič, Z. Kravanja, The two-level strategy for MINLP synthesis of process flowsheets under uncertainty, in: Computers and Chemical Engineering, Pergamon, 2000, pp. 195–201.
[15] J. Steimel, S. Engell, Conceptual design and optimization of chemical processes under uncertainty by two-stage programming, Comput. Chem. Eng. 81 (2015) 200–217, https://doi.org/10.1016/j.compchemeng.2015.05.016.
[16] M. Skiborowski, J. Wessel, W. Marquardt, Efficient optimization-based design of membrane-assisted distillation processes, Ind. Eng. Chem. Res. 53 (2014) 15698–15717, https://doi.org/10.1021/ie502482b.
[17] B. Scharzec, T. Waltermann, M. Skiborowski, A Systematic Approach towards Synthesis and Design of Pervaporation-Assisted Separation Processes, Chemie-Ingenieur-Technik 89 (2017) 1534–1549, https://doi.org/10.1002/cite.201700079.
[18] D.N. Chia, F. Duanmu, E. Sorensen, Single- and multi-objective optimisation of hybrid distillation-pervaporation and dividing wall column structures, Chem. Eng. Res. Des. 194 (2023) 280–305, https://doi.org/10.1016/j.cherd.2023.04.041.
[19] B. Scharzec, J. Holtkötter, J. Bianga, J.M. Dreimann, D. Vogt, M. Skiborowski, Conceptual study of co-product separation from catalyst-rich recycle streams in thermomorphic multiphase systems by OSN, Chem. Eng. Res. Des. 157 (2020) 65–76, https://doi.org/10.1016/j.cherd.2020.02.028.

[20] D. Rall, A.M. Schweidtmann, M. Kruse, E. Evdochenko, A. Mitsos, M. Wessling, Multi-scale membrane process optimization with high-fidelity ion transport models through machine learning, J. Membr. Sci. 608 (2020) 118208, https://doi.org/10.1016/j.memsci.2020.118208.
[21] M. Di Martino, S. Avraamidou, E.N. Pistikopoulos, A Neural Network Based Superstructure Optimization Approach to Reverse Osmosis Desalination Plants, Membranes 12 (2022), https://doi.org/10.3390/membranes12020199.
[22] P. Marchetti, M.F. Jimenez Solomon, G. Szekely, A.G. Livingston, Molecular separation with organic solvent nanofiltration: a critical review, Chem. Rev. 114 (2014) 10735–10806, https://doi.org/10.1021/cr500006j.
[23] R. Verbeke, FAIR and Open Data requires proper incentives and a shift in academic culture, Nat Water 1 (2023) 7–9, https://doi.org/10.1038/s44221-022-00012-1.
[24] S. van Buggenhout, G. Ignacz, S. Caspers, R. Dhondt, M. Lenaerts, N. Lenaerts, S. R. Hosseinabadi, I. Nulens, G. Koeckelberghs, Y. Ren, R.P. Lively, M. Rabiller-Baudry, K.M. Lim, N. Ghazali, J. Coronas, M. Abel, M. Wessling, M. Skiborowski, A. Oxley, S.J. Han, A. Livingston, Z. Yi, C. Gao, K. Guan, R.R. Gonzales, H. Matsuyama, S.N. Bettahalli, J.R. McCutcheon, F. Radmanesh, N.E. Benes, A. A. Tashvigh, Q. Fang, K. Zhang, G. Chen, W. Jin, Y. Zhang, C.-X. Zhang, M.-L. Liu, S.-P. Sun, A. Buekenhoudt, C. Zhao, B. van der Bruggen, J.F. Kim, L.C. Condes, M. T. Webb, M. Galizia, B. Alhazmi, L. Upadhyaya, S.P. Nunes, D.W. Kim, H. Schröter, U. Kragl, S. Störtte, A.J. Vorholt, P.Z. Culfaz-Emecen, M.-A. Pizzoccaro-Zilamy, L. Winnubst, A. Yushkin, A. Volkov, J. Chau, K.K. Sirkar, S. Lu, G. Szekely, I. Vankelecom, R. Verbeke, Open and FAIR data for nanofiltration in organic media: A unified approach, J. Membr. Sci. 713 (2025) 123356, https://doi.org/10.1016/j.memsci.2024.123356.
[25] G. Ignacz, A.K. Beke, G. Szekely, Data-driven investigation of process solvent and membrane material on organic solvent nanofiltration, J. Membr. Sci. 674 (2023) 121519, https://doi.org/10.1016/j.memsci.2023.121519.
[26] G. Ignacz, L. Bader, A.K. Beke, Y. Ghunaim, T. Shastry, H. Vovusha, M.R. Carbone, B. Ghanem, G. Szekely, Machine learning for the advancement of membrane science and technology: A critical review, J. Membr. Sci. 713 (2025) 123256, https://doi.org/10.1016/j.memsci.2024.123256.
[27] R. Goebel, T. Glaser, M. Skiborowski, Machine-based learning of predictive models in organic solvent nanofiltration: Solute rejection in pure and mixed solvents, Sep. Purif. Technol. 248 (2020) 117046, https://doi.org/10.1016/j.seppur.2020.117046.
[28] R. Goebel, M. Skiborowski, Machine-based learning of predictive models in organic solvent nanofiltration: Pure and mixed solvent flux, Sep. Purif. Technol. 237 (2020) 116363, https://doi.org/10.1016/j.seppur.2019.116363.
[29] S. Kaiser, S. Engell, An integrated approach to fast model-based process design: Integrating superstructure optimization under uncertainties and optimal design of experiments, Chem. Eng. Sci. 269 (2023) 118453, https://doi.org/10.1016/j.ces.2023.118453.
[30] R. Hernandez, J. Dreimann, A. Vorholt, A. Behr, S. Engell, Iterative Real-Time Optimization Scheme for Optimal Operation of Chemical Processes under Uncertainty: Proof of Concept in a Miniplant, Ind. Eng. Chem. Res. 57 (2018) 8750–8770, https://doi.org/10.1021/acs.iecr.8b00615.
[31] A.R. Gottu Mukkula, T.B. Riemer, A. Kühl, D. Vogt, S. Engell, Iterative real-time optimization of a reductive amination process in a thermomorphic multiphase system, Chem. Eng. Sci. 287 (2024) 119662, https://doi.org/10.1016/j.ces.2023.119662.
[32] A. Ahmad, R. Paulen, R. Valo, M. Fikar, S. Engell, Iterative real-time optimization of a membrane pilot plant, Control. Eng. Pract. 147 (2024) 105907, https://doi.org/10.1016/j.conengprac.2024.105907.
[33] J. Steimel, S. Engell, Optimization-based support for process design under uncertainty: A case study, AIChE Journal 62 (2016) 3404–3419, https://doi.org/10.1002/aic.15400.
[34] A. Wächter, L.T. Biegler, On the implementation of an interior-point filter line-search algorithm for large-scale nonlinear programming, Math. Program. 106 (2006) 25–57, https://doi.org/10.1007/s10107-004-0559-y.
[35] G. Franceschini, S. Macchietto, Model-based design of experiments for parameter precision: State of the art, Chem. Eng. Sci. 63 (2008) 4846–4872, https://doi.org/10.1016/j.ces.2007.11.034.
[36] H. Arellano-Garcia, J. Schöneberger, S. Körkel, Optimale Versuchsplanung in der Chemischen Verfahrenstechnik, Chemie-Ingenieur-Technik 79 (2007) 1625–1638, https://doi.org/10.1002/CITE.200700110.
[37] M. Bubel, J. Schmid, V. Kozachynskyi, E. Esche, M. Bortz, Sequential optimal experimental design for vapor-liquid equilibrium modeling, Chem. Eng. Sci. 300 (2024) 120566, https://doi.org/10.1016/j.ces.2024.120566.
[38] S. Recker, N. Kerimoglu, A. Harwardt, O. Tkacheva, W. Marquardt, On the integration of model identification and process optimization, Computer Aided Chemical Engineering 32 (2013) 1021–1026, https://doi.org/10.1016/B978-0-444-63234-0.50171-8.
[39] L. Fleitmann, J. Pyschik, L. Wolff, J. Schilling, A. Bardow, Optimal experimental design of physical property measurements for optimal chemical process simulations, Fluid Phase Equilib. 557 (2022) 113420, https://doi.org/10.1016/j.fluid.2022.113420.
[40] S. Kaiser, T. Menzel, S. Engell, Focusing experiments in the early phase process design by process optimization and global sensitivity analysis, in: 31st European Symposium on Computer Aided Process Engineering, Elsevier, 2021, pp. 899–904.
[41] A.J. Izenman, Linear Discriminant Analysis, in: G. Casella, S. Fienberg, I. Olkin, A. J. Izenman (Eds.), Modern Multivariate Statistical Techniques, Springer New York, New York, NY, 2008, pp. 237–280.
[42] H. Rinne, Taschenbuch der Statistik, fourth., vollst. überarb. und erw. Aufl., Deutsch, Frankfurt am Main, 2008.
[43] B.M. Greenwell, Pdp: an R package for constructing partial dependence plots, R Journal 9 (2017) 421–436. doi:10.32614/rj-2017-016, R J..
[44] J. Bianga, K.U. Künnemann, L. Goclik, L. Schurm, D. Vogt, T. Seidensticker, Tandem Catalytic Amine Synthesis from Alkenes in Continuous Flow Enabled by Integrated Catalyst Recycling, ACS Catal. 10 (2020) 6463–6472, https://doi.org/10.1021/acscatal.0c01465.
[45] J. Bianga, K.U. Künnemann, T. Gaide, A.J. Vorholt, T. Seidensticker, J. M. Dreimann, D. Vogt, Thermomorphic Multiphase Systems: Switchable Solvent Mixtures for the Recovery of Homogeneous Catalysts in Batch and Flow Processes, Chemistry – A, European Journal 25 (2019) 11586–11608, https://doi.org/10.1002/chem.201902154.
[46] A. Behr, Q. Miao, A new temperature-dependent solvent system based on polyethylene glycol 1000 and its use in rhodium catalyzed cooligomerization, J. Mol. Catal. A Chem. 222 (2004) 127–132, https://doi.org/10.1016/j.molcata.2004.05.039.
[47] A. Behr, G. Henze, L. Johnen, C. Awungacha, Advances in thermomorphic liquid/liquid recycling of homogeneous transition metal catalysts, J. Mol. Catal. A Chem. 285 (2008) 20–28, https://doi.org/10.1016/j.molcata.2008.01.021.
[48] S. Schlüter, K.U. Künnemann, M. Freis, T. Roth, D. Vogt, J.M. Dreimann, M. Skiborowski, Continuous co-product separation by organic solvent nanofiltration for the hydroaminomethylation in a thermomorphic multiphase system, Chem. Eng. J. 409 (2021) 128219, https://doi.org/10.1016/j.cej.2020.128219.
[49] W. Kortuz, S. Kirschtowski, A. Seidel-Morgenstern, C. Hamel, Kinetics of the Rhodium-Catalyzed Hydroaminomethylation of 1-Decene in a Thermomorphic Solvent System, Chemie-Ingenieur-Technik 94 (2022) 760–765, https://doi.org/10.1002/cite.202100180.
[50] J. Gross, G. Sadowski, Perturbed-chain SAFT: An equation of state based on a perturbation theory for chain molecules, Ind. Eng. Chem. Res. 40 (2001) 1244–1260, https://doi.org/10.1021/ie0003887.
[51] C. Nentwich, S. Engell, Surrogate modeling of phase equilibrium calculations using adaptive sampling, Comput. Chem. Eng. 126 (2019) 204–217, https://doi.org/10.1016/j.compchemeng.2019.04.006.
[52] P. Marchetti, A.G. Livingston, Predictive membrane transport models for Organic Solvent Nanofiltration: How complex do we need to be? J. Membr. Sci. 476 (2015) 530–553, https://doi.org/10.1016/j.memsci.2014.10.030.
[53] D. Fierro, A. Boschetti-de-Fierro, V. Abetz, The solution-diffusion with imperfections model as a method to understand organic solvent nanofiltration of multicomponent systems, J. Membr. Sci. 413-414 (2012) 91–101, https://doi.org/10.1016/j.memsci.2012.04.027.
[54] F. Huxoll, S. Schlüter, R. Budde, M. Skiborowski, M. Petzold, L. Böhm, M. Kraume, G. Sadowski, Phase Equilibria for the Hydroaminomethylation of 1-Decene, J. Chem. Eng. Data (2021), https://doi.org/10.1021/acs.jced.1c00561.
[55] Unisol Membrane Technology, UNISOL AMS NanoPro S-3014 Datasheet. http://www.amsmembrane.com/index.php/en/products/data-sheets (accessed 10 May 2024).
[56] Unisol Membrane Technology, UNISOL AMS NanoPro S-3012 Datasheet. http://www.amsmembrane.com/index.php/en/products/data-sheets (accessed 10 May 2024).
[57] K. Werth, P. Kaupenjohann, M. Skiborowski, The potential of organic solvent nanofiltration processes for oleochemical industry, Sep. Purif. Technol. 182 (2017) 185–196, https://doi.org/10.1016/j.seppur.2017.03.050.
[58] K.U. Künnemann, J. Bianga, R. Scheel, T. Seidensticker, J.M. Dreimann, D. Vogt, Process Development for the Rhodium-Catalyzed Reductive Amination in a Thermomorphic Multiphase System, Org. Process. Res. Dev. 24 (2020) 41–49, https://doi.org/10.1021/acs.oprd.9b00409.